

## Probing the Role of the Internal Disulfide Bond in Regulating Conformational Dynamics in Neuroglobin

Luisana Astudillo,<sup>†</sup> Sophie Bernad,<sup>‡§</sup> Valérie Derrien,<sup>‡§</sup> Pierre Sebban,<sup>‡§</sup> and Jaroslava Miksovská<sup>†\*</sup>

<sup>†</sup>Department of Chemistry and Biochemistry, Florida International University, Miami, Florida; <sup>‡</sup>University Paris-Sud, Laboratoire de Chimie-Physique, Faculté d'Orsay, Orsay cedex, France; and <sup>§</sup>CNRS, Orsay, France

**ABSTRACT** In this report, we demonstrate that the internal disulfide bridge in human neuroglobin modulates structural changes associated with ligand photo-dissociation from the heme active site. This is evident from time-resolved photothermal studies of CO photo-dissociation, which reveal a  $13.4 \pm 0.9 \text{ mL mol}^{-1}$  volume expansion upon ligand photo-release from human neuroglobin, whereas the CO dissociation from rat neuroglobin leads to a significantly smaller volume change ( $\Delta V = 4.6 \pm 0.3 \text{ mL mol}^{-1}$ ). Reduction of the internal disulfide bond in human neuroglobin leads to conformational changes (reflected by  $\Delta V$ ) nearly identical to those observed for rat Ngb. Our data favor the hypothesis that the disulfide bond between Cys<sup>46</sup> and Cys<sup>55</sup> modulates the functioning of human neuroglobin.

Received for publication 30 November 2009 and in final form 19 April 2010.

\*Correspondence: [miksovsk@fiu.edu](mailto:miksovsk@fiu.edu)

Here we report the influence of the internal disulfide bond on the conformational changes associated with the dissociation/rebinding of carbon monoxide to neuroglobin (Ngb). Ngb is a heme protein found predominantly in the brain tissue of mammals (1). Despite the very low sequence homology between Ngb and Mb (~16%), Ngb's 3D structure displays a characteristic globin fold with several unique features (2,3). In the resting state the Ngb's equilibrium is strongly displaced toward the oxidized form ( $\text{Fe}^{3+}$ ) rather than the reduced ( $\text{Fe}^{2+}$ ) one (3). Moreover, the heme iron in the ferric and ferrous protein is six-coordinated with His64 occupying the distal coordination site. The distal His can be readily displaced by  $\text{O}_2$  or CO. Indeed, Ngb binds  $\text{O}_2$  with relatively high affinity (1–2 Torr) (3). In vivo and in vitro studies have established that Ngb plays a role in the neuronal response to hypoxia and ischemia (4,5), although the molecular mechanism of the Ngb protective function remains unclear. Several plausible mechanisms have been proposed and are summarized in a recent review (5).

Wakasugi et al. (6) have reported that ferric Ngb binds to the  $\alpha$ -subunit of heterotrimeric G protein ( $G_{\alpha i}$ ) and inhibits the rate of GDP/GTP exchange, whereas the CO bound adduct does not show a significant affinity for  $G_{\alpha i}$ , suggesting for Ngb a role as an oxidative stress-responsive sensor. Glu<sup>53</sup> and Glu<sup>60</sup>, identified as possible interaction sites between Ngb and the  $G_{\alpha i}$  subunit (7), are located within a region formed by the CD-loop and the D-helix that undergoes a ligand-induced displacement in the crystal structure of the CO bound protein (3). Moreover, two cysteine residues (Cys<sup>46</sup> and Cys<sup>55</sup>) situated within the CD-loop/ H-helix region in human Ngb (hNgb) form an internal disulfide bond that increases Ngb's affinity for  $\text{O}_2$  by 10-fold. It is believed that this regulation occurs via disulfide bond induced alterations of the distal histidine dissociation rate (8). The internal disulfide bond in hNgb is conserved among different species with exception of rodent

Ngb's that carry a Cys<sup>46</sup> → Gly mutation. To investigate the role of the internal disulfide bond on structural changes associated with ligand dissociation/binding to Ngb, we have employed photoacoustic calorimetry (PAC) and transient absorption spectroscopy (TA) to determine time-resolved volume and enthalpy changes coupled to the CO photo-dissociation and the rate constants for CO rebinding to hNgb, hNgb reduced with DTT (hNgb<sup>red</sup>), Cys<sup>55</sup> → Ser hNgb mutant (Ser<sup>55</sup>hNgb), rat Ngb (rNgb), and Gly<sup>46</sup> → Cys rNgb mutant (Cys<sup>46</sup>rNgb) containing an engineered disulfide bond. Indeed, in the absence of a 3D structure for hNgb with a native disulfide bond, there is very little information regarding the impact of the internal disulfide bond on the conformational state of Ngb. The absorption spectra of ferric, ferrous and CO bound adducts of rNgb, hNgb, and mutants are superimposed, indicating that mutation of residues in position 46 or 55 does not modify the heme pocket (data not shown). A representative PAC trace for CO photo-dissociation from hNgb and the reference compound, Fe(III) tetraphenylsulfonate porphyrin (Fe4SP), are shown in Fig. 1. The sample and reference acoustic traces overlay in phase indicating the absence of volume/enthalpy changes in hNgb sample on a time-scale between ~50 ns and ~5  $\mu\text{s}$ , suggesting that the CO photorelease occurs with  $\tau < 50 \text{ ns}$ . Likewise, no phase-shift between the sample and reference trace was detected for the ligand dissociation from all samples studied (data not shown). The volume and enthalpy changes taking place within 50 ns upon ligand photo-release were determined from a plot of the ratio of sample amplitude (S) to reference amplitude (R) scaled to the photon energy at 532 nm ( $E_{\text{hv}}$ ) versus the temperature dependent factor ( $C_p \rho / \beta$ ) (Fig. 2), where

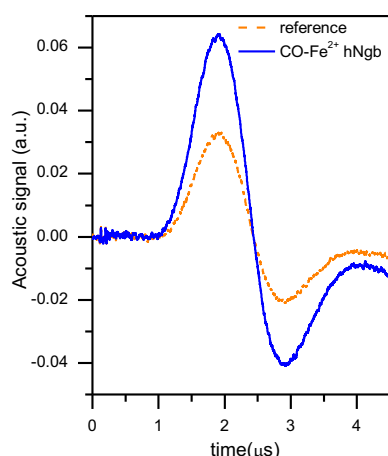


**FIGURE 1** PAC signal for CO photo-dissociation from hNgb and for the reference, Fe(III)4SP, at 20°C. Conditions: Sample: 20  $\mu\text{M}$  Fe<sup>2+</sup>hNgb in 50 mM Tris buffer pH 7.0 and 1 mM CO.

$C_p$  is the heat capacity,  $\rho$  the density, and  $\beta$  the expansion coefficient (9). For events that occur with quantum yield ( $\Phi$ ) less than unity, the reaction volume and enthalpy changes are obtained by scaling to  $\Phi$  (9). The thermodynamic parameters for CO photo-release from Ngb, obtained using  $\Phi = 0.68$  (10), are listed in Table 1.  $\Phi$  for the bimolecular CO dissociation is the same for rNgb and hNgb based upon a comparison of the amplitude of the absorbance changes upon ligand photo-release at 436 nm (data not shown).

Similar values of enthalpy changes ( $\sim 19 \text{ kcal mol}^{-1}$ ) were found for all samples. This value is close to the enthalpy change determined by PAC for CO photo-release from heme model complexes with imidazole as a proximal ligand ( $\Delta H = 17 \text{ kcal mol}^{-1}$ ) (9), suggesting that the observed enthalpy change reflects the cleavage of the Fe-CO bond, whereas the concomitant structural changes (see below) are predominantly entropy driven. The reaction volume change corresponds to differences in the partial molar volumes of

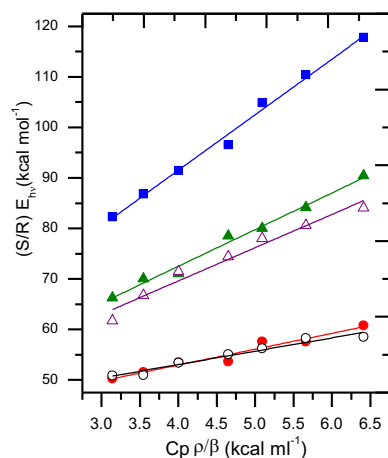


**FIGURE 2** Plot of  $(S/R)E_{hv}$  for CO photo-dissociation from hNgb (solid squares), rNgb (solid circles), Cys46rNgb (solid triangles), Ser55hNgb (open triangles), hNgb<sup>red</sup> (open circles).

**TABLE 1** Reaction volume and enthalpy changes determined for CO photo-dissociation from Ngb.

	$\Delta V \text{ (mL mol}^{-1}\text{)}$	$\Delta H \text{ (kcal mol}^{-1}\text{)}$
hNgb	$13.4 \pm 0.9$	$20 \pm 4$
hNgb <sup>red</sup>	$4.4 \pm 0.3$	$19 \pm 2$
Ser55hNgb	$7.1 \pm 0.7$	$19 \pm 2$
rNgb	$4.6 \pm 0.3$	$19 \pm 2$
Cys46rNgb	$10.3 \pm 0.6$	$19 \pm 4$

the products and reactants and can be expressed as:  $\Delta V = V_{\text{CO}} + V_{\text{Ngb}} - V_{\text{CONgb}}$ , where  $V_{\text{CO}}$  is the partial molar volume of CO ( $30 \text{ mL mol}^{-1}$ ) (9)), and  $V_{\text{Ngb}}$  and  $V_{\text{CONgb}}$  correspond to the partial molar volume of the ligand free, five-coordinated Ngb, and CO bound Ngb, respectively. Therefore, CO photo-dissociation from hNgb is associated with the overall structural volume change ( $\Delta V_{\text{str}} = V_{\text{Ngb}} - V_{\text{CONgb}}$ ) of  $-17 \text{ mL mol}^{-1}$ . A more negative structural volume change ( $-25 \text{ mL mol}^{-1}$ ) was detected for rNgb and hNgb<sup>red</sup>. Engineering of the disulfide bond into rNgb structure in Cys<sup>46</sup>rNgb mutant leads to the structural volume change approaching to that of hNgb ( $\Delta V_{\text{str}} = -20 \text{ mL mol}^{-1}$ ) whereas Ser55hNgb mutant displays a more negative volume change than hNgb WT ( $\Delta V_{\text{str}} = -22 \text{ mL mol}^{-1}$ ).

Recently, kinetics for CO migration between Ngb internal cavities were reported to occur on 100 ns timescale (11). Those kinetics were not resolved in PAC measurements due to the very low fraction ( $< 10\%$ ) of “CO trapped” intermediates. The fast ligand photo-release thermodynamics observed in PAC indicates that the major fraction of CO escapes from protein through a direct pathway (either permanent or transitory) linking the Ngb heme binding pocket with the surrounding solvent. To further investigate the impact of the internal disulfide bond on the conformational dynamics of ligand binding in Ngb, the rate constants for CO binding to the heme iron were also determined using time-resolved absorption spectroscopy (Fig. 3). As with other six-coordinated hemoglobins, CO rebinding to Ngb is a biphasic process with the first phase reflecting CO rebinding to a population of five-coordinate deoxy Ngb and the slow phase

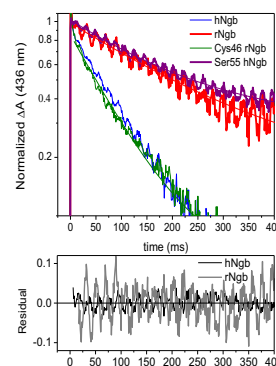


**FIGURE 3** TA traces for the slow phase of the CO rebinding to Ngb. Conditions: 40  $\mu\text{M}$  Ngb, 50 mM Tris pH 7.0, 0.1 mM CO at 35°C. The data were normalized to the amplitude for the slow phase. The systematic oscillation is due to the PMT noise.

corresponding to a population of protein in which the intrinsic ligand (i.e., His<sup>64</sup>) has rebound (8). The rate for the second process is governed by the thermal dissociation of distal histidine side chain from the heme iron. The rate constants determined for the fast and the slow phases are summarized in Table 2. The presence of the disulfide bond only moderately impacts the observed rate constants for the fast process and the reported values match well those determined previously (8). Our data show that the rate constant for CO rebinding to six - coordinate heme is two times smaller for samples missing the internal disulfide bond (rNgb and Ser<sup>55</sup>hNgb) compared to hNgb and Cys<sup>46</sup>rNgb in agreement with the previously published data (8).

The PAC results clearly indicate that the presence of the internal disulfide bond modulate overall structural changes associated with the transition from six-coordinate CO bound Ngb to five-coordinate deoxyNgb by  $\sim 8 \text{ mL mol}^{-1}$ . An overlay of the structure of the ferrous and CO bound rNgb reveals that ligand binding to the heme iron leads to the repositioning of the heme prosthetic group, reshaping of the internal cavity, and displacement of structural elements including the EF- and CD-loops (3). Molecular dynamic studies have suggested that the disulfide bridge restrict the flexibility of Ngb structure including CD-loop region and A, C, and E helices and modulate the volume of internal cavities (12,13). In addition, the heme sliding mechanism proposed in rNgb structure was suggested to be protein dependent (12,13,14). Such restricted structural dynamics due to the disulfide bridge may then translate into the smaller overall structural volume changes determined for hNgb relative to rNgb or hNgb<sup>red</sup>. Ser<sup>55</sup> in hNgb structure may form a hydrogen bond with Cys<sup>46</sup> and stabilize the CD loop resulting in smaller structural volume change determined for Ser<sup>55</sup>hNgb compared to hNgb<sup>red</sup>. Considering the high sequence identity between hNgb and rNgb (94%), the fact that the structural volume change observed for the Cys<sup>46</sup>rNgb mutant does not match that for hNgb is somewhat surprising. This result points out that other factors, in addition to the disulfide bond, may contribute to the difference between the overall volume changes measured for hNgb and rNgb.

**TABLE 2 The rate constant for the fast phase ( $k_{\text{fast}}$ ) and slow phase ( $k_{\text{slow}}$ ) of CO rebinding to Ngb. Conditions: 40  $\mu\text{M}$  Ngb, 50 mM Tris pH 7.0.  $k_{\text{fast}}$  was determined at 1 mM CO and 20°C and  $k_{\text{slow}}$  at 0.1 mM CO and 35°C to increase the yield of bis histidine form of Ngb.**

	$k_{\text{fast}} (\mu\text{M}^{-1}\text{s}^{-1})^*$	$k_{\text{slow}} (\mu\text{M}^{-1}\text{s}^{-1})$
hNgb	62	0.100
Ser55hNgb	65	0.052
rNgb	70	0.051
Cys46rNgb	45	0.105

\*An additional phase with rate constant of  $10 \text{ mM}^{-1}\text{s}^{-1}$  and amplitudes of 10% for hNgb and rNgb, and 38% for Cys46rNgb was observed for CO rebinding to five-coordinate heme. The error of the rate constant is 10% of the observed value.

In summary, the data presented here illustrates that the overall volume change associated with the CO dissociation varies between hNgb and rNgb and that the presence of the internal disulfide bond modulates, to some extent, the magnitude of the overall structural changes in Ngb upon ligand binding/release. On the other hand, the presence of the disulfide bond fully contributes to the increased rate constant for distal histidine dissociation in hNgb relative to rNgb. Moreover, CO escape from the protein matrix is significantly faster in Ngb relative to myoglobin implying a distinct mechanism of ligand-protein interaction between these classes of proteins leading to a unique function of Ngb in neuronal tissue as compared to myoglobin.

## ACKNOWLEDGMENTS

This work was partially supported by the American Heart Association (J.M.), the University Paris-Sud 11, and the Centre National de la Recherche Scientifique (P.S.).

## REFERENCES and FOOTNOTES

- Burmester, T., B. Weich, ..., T. Hankeln. 2000. A vertebrate globin expressed in the brain. *Nature*. 407:520–523.
- Pesce, A., S. Dewilde, ..., M. Bolognesi. 2003. Human brain neuroglobin structure reveals a distinct mode of controlling oxygen affinity. *Structure*. 11:1087–1095.
- Vallone, B., K. Nienhaus, ..., G. U. Nienhaus. 2004. The structure of carbonmonoxy neuroglobin reveals a heme-sliding mechanism for control of ligand affinity. *Proc. Natl. Acad. Sci. USA*. 101:17351–17356.
- Sun, Y., K. Jin, ..., D. A. Greenberg. 2003. Neuroglobin protects the brain from experimental stroke in vivo. *Proc. Natl. Acad. Sci. USA*. 100:3497–3500.
- Greenberg, D. A., K. Jin, and A. A. Khan. 2008. Neuroglobin: an endogenous neuroprotectant. *Curr. Opin. Pharmacol.* 8:20–24.
- Wakasugi, K., T. Nakano, and I. Morishima. 2003. Oxidized human neuroglobin acts as a heterotrimeric Galpha protein guanine nucleotide dissociation inhibitor. *J. Biol. Chem.* 278:36505–36512.
- Kitatsuji, C., M. Kuroguchi, ..., K. Wakasugi. 2007. Molecular basis of guanine nucleotide dissociation inhibitor activity of human neuroglobin by chemical cross-linking and mass spectrometry. *J. Mol. Biol.* 368:150–160.
- Hamdane, D., L. Kiger, ..., M. C. Marden. 2003. The redox state of the cell regulates the ligand binding affinity of human neuroglobin and cytoglobin. *J. Biol. Chem.* 278:51713–51721.
- Miksovskaya, J., and R. W. Larsen. 2003. Structure-function relationships in metalloproteins. In *Methods in Enzymology: Biophotonics*, G. Marriott, and I. Parker, ed. 360:302–323.
- Kriegel, J. M., A. J. Bhattacharyya, ..., G. U. Nienhaus. 2002. Ligand binding and protein dynamics in neuroglobin. *Proc. Natl. Acad. Sci. USA*. 99:7992–7997.
- Abbruzzetti, S., S. Faggiano, ..., C. Viappiani. 2009. Ligand migration through the internal hydrophobic cavities in human neuroglobin. *Proc. Natl. Acad. Sci. USA*. 106:18984–18989.
- Bocahut, A., S. Bernad, ..., S. Sacquin-Mora. 2009. Relating the diffusion of small ligands in human neuroglobin to its structural and mechanical properties. *J. Phys. Chem. B*. 113:16257–16267.
- Nadra, A. D., M. A. Martí, ..., D. A. Estrin. 2008. Exploring the molecular basis of heme coordination in human neuroglobin. *Proteins*. 71:695–705.
- Anselmi, M., M. Brunori, ..., A. Di Nola. 2007. Molecular dynamics simulation of deoxy and carboxy murine neuroglobin in water. *Biophys. J.* 93:434–441.